The nonlinear saturation of beam-driven instabilities: Theory and experiment

W. W. Heidbrink, H. H. Duong, J. Manson, E. Wilfrid, and C. Oberman*
Department of Physics, University of California, Irvine, California 92717

E. J. Strait
General Atomics, P.O. Box 85608, San Diego, California 92186-9784

(Received 14 December 1992; accepted 8 March 1993)

Intense fast-ion populations created by neutral-beam injection into a tokamak can destabilize toroidicity-induced Alfvén eigenmodes (TAE modes) or internal kink modes. Experimentally, these modes stabilize when fast ions are ejected from the plasma, producing a cycle of relaxation oscillations about the marginal stability point. A pair of coupled differential equations describes this cycle. This simple theoretical formalism successfully describes the cycles observed during TAE experiments in DIII-D [*Plasma Physics Controlled Nuclear Fusion Research, 1986* (International Atomic Energy Agency, Vienna, 1987), Vol. 1, p. 159].

I. INTRODUCTION

In tokamaks, the confinement of superthermal ions is usually superior to the confinement of thermal particles, and "fast" ions generally thermalize within the plasma.[1] If the density of fast ions is sufficiently large, however, the free energy in the fast-ion population can drive normal modes of the background plasma unstable and degrade the fast-ion confinement. Losses associated with collective instabilities can damage the walls of the device and can reduce the heating efficiency. In particular, instabilities driven by alpha particles may prevent ignition in a deuterium–tritium (D–T) reactor.

Several potentially dangerous fast-ion-driven instabilities exist. The "fishbone" instability was first observed[2] during perpendicular beam injection into the Princeton Divertor Experiment (PDX) and was subsequently seen in many tokamaks.[1] This is a relatively low-frequency mode [$\mathcal{O}$(10 kHz)] with the structure of an $n=1$ internal kink (n is the toroidal mode number). A related instability, which we call the "sawbone" instability, also has the structure of an $n=1$ internal kink, but the mode amplitude collapses relatively suddenly (similar to the crash phase of the "sawtooth" instability[3]) and the frequency spectrum contains higher-frequency components of $\mathcal{O}$(100 kHz). Sawbones were observed[4] during tangential injection into the Princeton Beta Experiment (PBX) and also in several other tokamaks.[1] Alfvén modes are also dangerous. Toroidicity-induced Alfvén eigenmodes (TAE) are observed in the Tokamak Fusion Test Reactor (TFTR),[5] in (Doublet III-D),[6] and may have been observed in other tokamaks.[1] These are modes with frequencies of $\mathcal{O}$(100 kHz) that have toroidal mode numbers between $n=1$–10 and a ballooning structure poloidally. Other instabilities, such as global Alfvén eigenmodes (GAE),[7] ellipticity-induced Alfvén eigenmodes (EAE),[8] and kinetic ballooning modes[9] may be important in existing and future devices.

All these modes are destabilized by the fast-ion population. Since the density of the background plasma is generally much greater than the fast-ion density, the frequency and spatial structure of the mode are determined primarily by the thermal plasma. In the absence of fast ions, the modes are weakly damped, with the damping determined by properties of the plasma (such as the magnetic shear and the temperature and density profiles of the various thermal species). Theoretically, the fast-ion drive term depends upon the velocity and spatial distribution of the fast ions, and upon their number density. A generic drive term is of the form $\gamma_f = \mathcal{N}\mathcal{S}\mathcal{F}$, where $\mathcal{N}$ depends upon the number of fast ions, $\mathcal{S}$ depends upon their spatial distribution, and $\mathcal{F}$ depends upon their velocity distribution. For example, for TAE modes the fast-ion drive term is of the form[10–12]

$$\gamma_f \propto \beta_f \left(\frac{\omega_{*f}}{\omega} - 1 \right) F(\mathbf{v}), \tag{1}$$

where γ_f is the growth rate associated with the fast-ion drive, β_f is the ratio of the fast-ion kinetic energy to magnetic field energy, ω_{*f} is the fast-ion diamagnetic frequency, ω is the mode frequency, and $F(\mathbf{v})$ is a function that depends upon the fraction of fast ions with parallel velocities comparable to the phase velocity of the mode. According to Eq. (1), the drive term for TAE modes depends upon the product of the density of fast ions (β_f), their spatial distribution (ω_{*f}), and the fraction of resonant particles (F). The drive term for other fast-ion-driven instabilities is qualitatively similar.

There are several mechanisms that could determine the saturation amplitude of an unstable fast-ion-driven mode. Nonlinear coupling to stable modes could provide additional damping, but the modes under consideration tend to be separated in frequency ω and wave vector $\mathbf{k}$ from other modes, so this mechanism is likely to be relatively weak. The instability could change the properties of the background plasma and thereby modify the linear damping terms. The time scale for changes in the temperature or current profiles is relatively long, however, so this mechanism is very improbable. Alternatively, frequency shifts introduced by nonlinearities could increase coupling to damped modes, thereby enhancing the damping. However,

*Deceased.

 0899-8221/93/5(7)/2176/11/$6.00

the most likely scenario is that nonlinear saturation of fast-ion-driven modes is caused by modification of one or more of the factors that compose the drive term. In previous studies of the saturation of TAE modes, modification of the spatial gradient[13] and of the velocity distribution[14,15] were explored as potential saturation mechanisms. Saturation via particle loss was originally explored as part of theoretical studies of the fishbone instability.[16,17]

In this paper, we assume that the dominant saturation mechanism is the loss of fast ions, i.e., that saturation is achieved through reduction in $\mathcal{N}$ of the drive term. This hypothesis is motivated by the experimental observation that large numbers of beam ions are expelled from the plasma during fishbone[1,2,18] and TAE[19,20] activity and that saturation is coincident with the fast-ion losses. Another important experimental observation is that the saturation mechanism is a powerful one that tends to clamp the fast-ion beta near the point of marginal stability.[19,21] This observation tends to preclude nonlinear couplings or frequency shifts as potential saturation mechanisms. Although changes in the spatial gradient and velocity distribution may occur, only fast-ion loss is firmly established experimentally. We find that the observed growth and saturation of the TAE mode in DIII-D is consistent with the hypothesis that particle loss is the dominant saturation mechanism.

A complete theory of mode saturation requires careful kinetic analysis of the nonlinear interaction of particles with the excited modes. In this paper we adopt a simpler, semiempirical approach. We begin by generalizing and extending the heuristic model proposed by Coppi *et al.*[17] to other beam-driven instabilities (Sec. II). A more complete solution of the equations is given (Sec. II) and the relationship of the solution to measured quantities is considered (Sec. III). The model is then applied to experimentally observed cycles of instability in the DIII-D tokamak[22] (Sec. IV). The model is able to reproduce the essential features of the magnetics and neutron measurements, and gives reasonable values for the linear mode damping rate (Sec. V). We conclude that fast-ion loss controls mode saturation in present experiments and will probably dominate nonlinear saturation in future devices as well (Sec. VI).

II. THEORY

The linear stability of a beam-driven mode such as the TAE mode is determined by a competition between the fast-ion drive term γ_f and the damping of the background plasma, which is characterized by a "growth rate," $-\gamma_{\rm damp}$. Call the mode amplitude A. Then, if nonlinear couplings are negligible, the time evolution of A is

$$\frac{dA}{dt}=(\gamma_f-\gamma_{\rm damp})A. \tag{2}$$

Theoretically, the drive term for fishbones, TAE modes, and other beam-driven modes is linearly proportional to the number of beam ions. Experimentally, the number of beam ions N_b appears to oscillate about the (linear) marginal stability point. We therefore rewrite the drive term as

$$\gamma_f=\frac{N_b}{\bar{N}_b}\bar{\gamma}_f,$$

where $\bar{N}_b$ is the number of beam ions at marginal stability and $\bar{\gamma}_f=\gamma_{\rm damp}$ is the drive term evaluated at marginal stability. With these definitions, Eq. (2) becomes

$$\frac{dA}{dt}=\gamma_{\rm damp}\left(\frac{N_b}{\bar{N}_b}-1\right)A. \tag{3}$$

Growth of the instability induces fast-ion loss. Several loss mechanisms are possible. Resonant convective transport ("mode-particle pumping") causes losses that are linearly proportional to the mode amplitude A.[23] Another resonant loss process that may be of importance for TAE modes is velocity-space transport across the passed/trapping boundary onto an unconfined banana orbit; this mechanism is also calculated to result in losses that are linearly proportional to the mode amplitude A.[24] Stochastic orbit loss due to island overlap in phase space is another potential loss mechanism; in this case, diffusive losses that scale as A^2 are predicted.[24] The destruction of magnetic surfaces at large mode amplitudes could result in losses with an even stronger functional dependence upon mode amplitude.

In a stable plasma, the beam number N_b is determined by the competition between beam fueling and Coulomb drag. In a plasma with strong beam-driven instabilities, mode-induced loss joins Coulomb drag as an important loss mechanism. If the period between magnetohydrodynamic (MHD) bursts T is short compared to the characteristic thermalization time $\tau_{\rm th}$ and the losses at each burst are relatively small ($\Delta N_b/\bar{N}_b\ll 1$), then the steady-state losses associated with Coulomb drag are simply related to the thermalization time and the *average* number $\bar{N}_b$ by $dN_b/dt\propto -\bar{N}_b/\tau_{\rm th}$. Under these conditions, which are usually satisfied in practice, we can define an effective fueling rate S,

$$S\simeq P_b/E_b-\bar{N}_b/\tau_{\rm th}, \tag{4}$$

that is approximately constant in time. (Here P_b is the beam power and E_b is the injection energy.)

To account for the various possible loss mechanisms, we assume that the losses are proportional to A^ν, where $\nu=1$ for resonant losses and $\nu=2$ for diffusive losses. The equation for the time evolution of the beam number becomes

$$\frac{dN_b}{dt}=S-\gamma_{\rm loss}\bar{N}_bA^\nu. \tag{5}$$

The constant $\gamma_{\rm loss}$ is a normalization factor that depends upon the efficacy and type of the loss mechanism, and upon the units of the mode amplitude A. (In the experimental section of this paper, we normalize the mode amplitude to the poloidal field B_θ, but other normalizations are also possible.) Strictly speaking, the loss term should be proportional to N_b rather than the average number $\bar{N}_b$, but

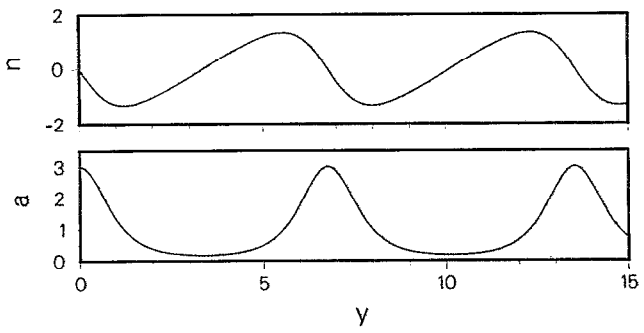

FIG. 1. Numerical solution of Eqs. (9) and (10) for $a_m=3.0$. For $\nu=1$, this solution reproduces the PDX fishbone cycle (Fig. 1 of Ref. 2).

use of the average value only modifies the losses by a few percent for realistic parameters. The validity of our model is discussed in more detail in Sec. V.

Equations similar to Eqs. (3) and (5) were first derived in Refs. 16, 17, and 25. The equations resemble the equations Volterra introduced to describe two species that live in a predator–prey relationship.[26] In our case, the mode amplitude acts as the "predator" that preys upon the population of beam ions.

Equations (3) and (5) constitute a pair of coupled first-order, ordinary differential equations in the variables A and N_b. The use of dimensionless variables simplifies the analysis. Introduce a normalized time y,

$$y\equiv\left(\frac{S}{\bar{N}_b}\nu\gamma_{\rm damp}\right)^{1/2}t, \tag{6}$$

a normalized beam number n that oscillates about the marginal stability point at $n=0$,

$$n\equiv\frac{N_b-\bar{N}_b}{\bar{N}_b}\sqrt{\frac{\bar{N}_b}{S}}\nu\gamma_{\rm damp}, \tag{7}$$

and a normalized mode amplitude a,

$$a\equiv\left(\gamma_{\rm loss}\frac{\bar{N}_b}{S}\right)A^{\nu}. \tag{8}$$

Equations (3) and (5) then become

$$\frac{da}{dy}=na \tag{9}$$

and

$$\frac{dn}{dy}=1-a. \tag{10}$$

The solution to these equations is periodic in the normalized time y. Without loss of generality, we can select as initial conditions $a=a_m\geqslant 1$ and $n=0$ at $y=0$. The solution then depends upon a single parameter: the maximum amplitude a_m (the initial condition). Graphs of the solution for a particular case are shown in Fig. 1. Initially, the amplitude $a>1$, so the beam number n decreases, since $1-a<0$ [Eq. (10)]. Since n is negative, the mode amplitude a, which is always greater than zero, decays according to Eq. (9). The number of beam ions reaches its minimum value as the amplitude passes through $a=1$. At this point, n begins to increase, but the amplitude continues to decay until n passes through zero. At this point $na>0$, so the amplitude begins to grow [Eq. (9)]. The growth phase continues until the amplitude crosses unity from below and dn/dy becomes negative. The maximum amplitude is reached when n passes through zero, and the cycle repeats.

The solution of the above equations was previously discussed by Coppi *et al.*[17] [Note that there are errors in their Eqs. (C8) and (C10).[27]] However, a more transparent treatment is facilitated by observing that, with the identifications $p=n$ and $q=\ln a$, Eqs. (9) and (10) assume the form of Hamiltons's equations in the position coordinate q and the momentum coordinate p. The Hamiltonian H, which is conserved[28] and equals the energy E, is given by

$$H=\tfrac{1}{2}n^2+a-\ln a=E. \tag{11}$$

Noting that $a=a_m$ at $n=0$, we find that the number of beam ions is related to the amplitude by

$$n=\pm\sqrt{2}\sqrt{a_m-a-\ln(a_m/a)}, \tag{12}$$

and the total change in n during the cycle $\Delta n\equiv n_{\rm max}-n_{\rm min}$ is

$$\Delta n=2^{3/2}\sqrt{a_m-1-\ln a_m}. \tag{13}$$

According to Eq. (12), the decay and growth phases of the cycle are symmetric in the normalized time y, while n is antisymmetric. From the expression for the energy we also find that the minimum amplitude $a_{\rm min}$ is related to the maximum amplitude by

$$a_{\rm min}-\ln a_{\rm min}=a_m-\ln a_m. \tag{14}$$

For Hamilton's equations, the period Y is related to the action J and energy E by $Y=dJ/dE$, where the action is $J=\oint p\,dq$. Differentiation of J yields an explicit expression for the period,

$$Y=\sqrt{2}\int_{a_{\rm min}}^{a_m}\frac{da}{a\sqrt{a_m-a-\ln(a_m/a)}}. \tag{15}$$

It is possible to show that for weak instability ($a_m\to 1$), the period $Y\to 2\pi$. Only for the special case of $a_m=1$ (the limit point of the cycle) is a steady-state solution obtained. The numerical solution for Y as a function of a_m is graphed in Fig. 2. The period Y increases gradually with increasing mode amplitude a_m. This behavior arises from the competition between two opposing tendencies. Large mode amplitude occurs when the effective fueling $S/\bar{N}_b$ is strong, resulting in explosive growth of the mode. Strong fueling tends to shorten the recovery between bursts, but large amplitudes cause large fast-ion losses, which tends to lengthen the period. Since the latter effect is stronger, the period increases weakly with increasing mode amplitude.

III. RELATIONSHIP TO MEASURED QUANTITIES

Having solved the equations, we next consider the relationship of the solution to experimentally measured quantities. Figure 3 shows typical neutron and magnetic

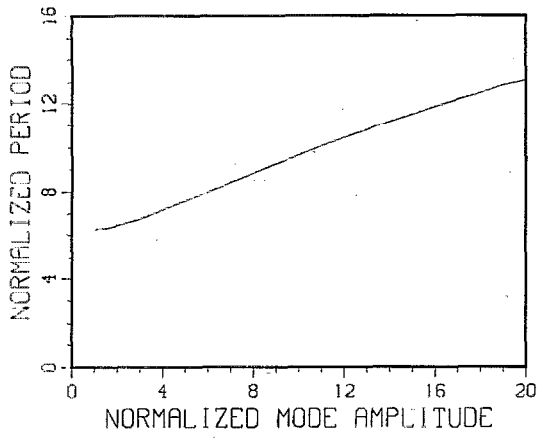

FIG. 2. The normalized period Y versus the normalized mode amplitude a_m.

data during a relaxation cycle of a TAE mode in DIII-D. In this discharge, deuterium beams are injected into a deuterium plasma. For these conditions, the 2.5 MeV neutron emission is dominated by beam–plasma reactions (>70%), with a much smaller contribution from beam–beam reactions and negligible contribution from thermonuclear reactions. For beam–plasma reactions, the neutron emission I_n is linearly proportional to the total number of beam ions in the plasma N_b,[1]

$$I_n \simeq \hat{n}_d N_b \langle \sigma v \rangle, \tag{16}$$

where $\hat{n}_d$ is the deuterium density in the plasma center and $\langle \sigma v \rangle$ is the fusion reactivity (which depends strongly upon the injection energy and weakly upon the background plasma parameters). In principle, a redistribution of beam ions to regions of lower deuterium density may cause a reduction in neutron emission. Edge measurements indicate that beam ions are expelled from the plasma by fishbones[29,30] and TAE[19,20] activity, however, so we assume

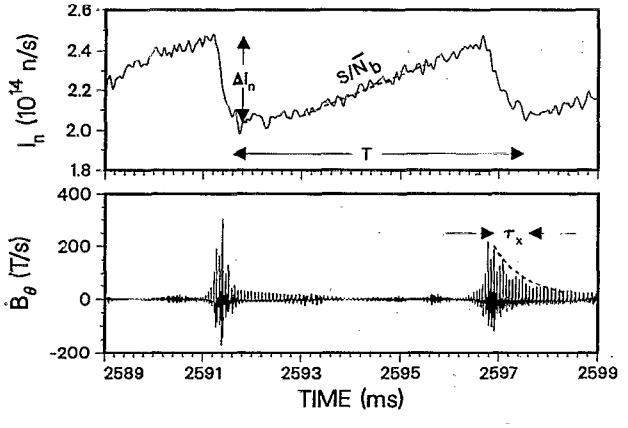

FIG. 3. Time evolution of the neutron emission and of the signal from a magnetic pickup loop (digitally filtered to pass frequencies above 70 kHz) for the discharge with TAE activity shown in Fig. 6. The change in beam number ΔN_b is inferred from the drop in neutron emission ΔI_n. The effective fueling rate $S/\bar{N}_b$ is obtained from the slope of the neutron emission between bursts. The $1/e$ rise and fall times τ_x are obtained from the Mirnov signal. The period T is the time between bursts.

that the reduction in neutron emission is due to a reduction in the number of beam ions, $\Delta N_b/\bar{N}_b = \Delta I_n/\bar{I}_n$ (Fig. 3). The rate of effective beam fueling is obtained from the slope of the neutron emission during the period between beam bursts (when the beam-ion losses are negligible), using the relation $S/\bar{N}_b = (dI_n/dt)/\bar{I}_n$ (Fig. 3).

The mode amplitude is inferred from measurements of the magnetic fluctuations at the plasma edge $\tilde{B}_\theta$. Theoretically, the amplitude of greatest interest is the displacement within the plasma, but this is not routinely measured on most tokamaks. If the mode structure is constant in time, the edge fluctuations are linearly proportional to the central displacement, and we assume that this is the case. For the fishbone instability, the frequency of the mode often changes in time,[2] so it is necessary to distinguish between the measured signal $\dot{B}_\theta$ and the mode amplitude $\tilde{B}_\theta$; corrections for changes in frequency are unimportant for TAE modes. Both the "rise" time and "fall" time are well-defined quantities experimentally (Fig. 3). These quantities are obtained from the envelope of the magnetics signal, assuming that the mode grows and decays approximately exponentially with a time constant τ_x.

The period of the relaxation cycle T is readily obtained from either the neutron or the magnetics signal (Fig. 3).

With the use of Eqs. (6)–(8), the measured quantities are related to the theoretical quantities by

$$\frac{\Delta n}{Y} = \frac{\Delta I_n}{\bar{I}_n} \frac{1}{T(S/\bar{N}_b)} \tag{17}$$

and by

$$\frac{\nu\tau}{Y} = \frac{\tau_x}{T}, \tag{18}$$

where τ is the dimensionless $1/e$ decay "time" of the normalized amplitude a. The quantities $\Delta n/Y$ and τ/Y are plotted as a function of a_m in Fig. 4. These graphs and the formulas for $\Delta n/Y$ and $\nu\tau/Y$ allow us to relate the measured cycle to the solution (or solutions) of the model equations [Eqs. (3) and (5)] that best fits the data. First we use Fig. 4(b) to find the value of a_m that is consistent with the measured value of $\Delta n/Y$. Next, a_m is used in Fig. 4(a) to find τ/Y. Comparison with the measured value of τ_x/T then yields the loss parameter ν through the formula $\nu = (\tau_x/T)/(\tau/Y)$.

As a specific example, consider the PDX fishbone cycle published in Fig. 1 of Ref. 2. The first nine fishbone bursts in the cycle are similar but not identical. The drop in neutron emission for these nine events is $\Delta I_n/I_n = 0.32 \pm 0.06$ and the period between bursts is $T = 2.7 \pm 0.3$ msec. From the rate of rise of the neutron emission between bursts we obtain a fueling rate of $S/\bar{N}_b = 230 \pm 20$ sec^{-1}. The observed rise and decay times of the Mirnov signal give $\tau_x = 0.53 \pm 0.06$ msec. Substitution of these data into Eqs. (17) and (18) gives a normalized neutron drop of $\Delta n/Y$

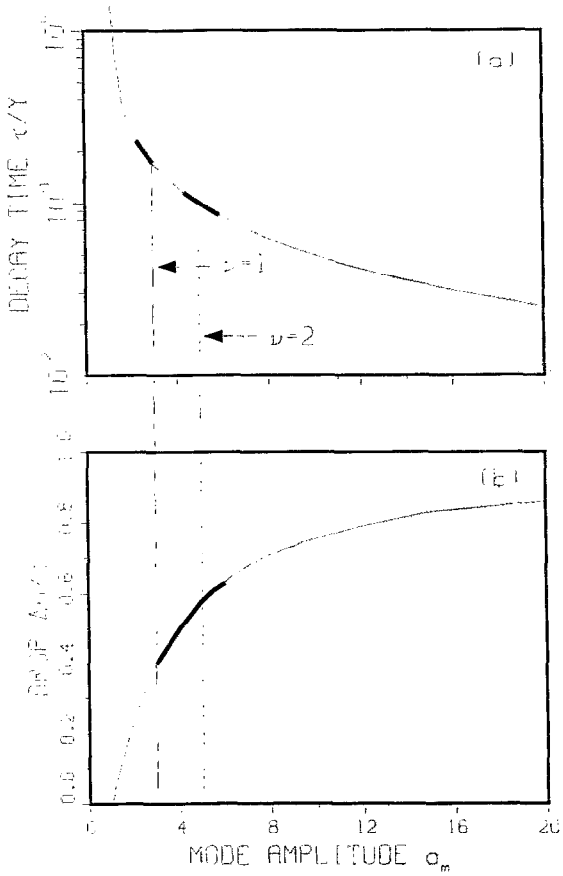

FIG. 4. Normalized decay time τ/Y and normalized drop in the number of beam ions $\Delta n/Y$ versus the maximum normalized mode amplitude a_m. The darkened region indicates the measured value of $\Delta n/Y$ (one standard deviation) for the PDX fishbone cycle; the measured value of τ/Y for $\nu=1$ and for $\nu=2$ are also shown. For $\nu=1$, $a_m=3$ is consistent with the measured values of τ_x/T and $\Delta n/Y$, while for $\nu=2$, $a_m=5$ fits the data (vertical lines).

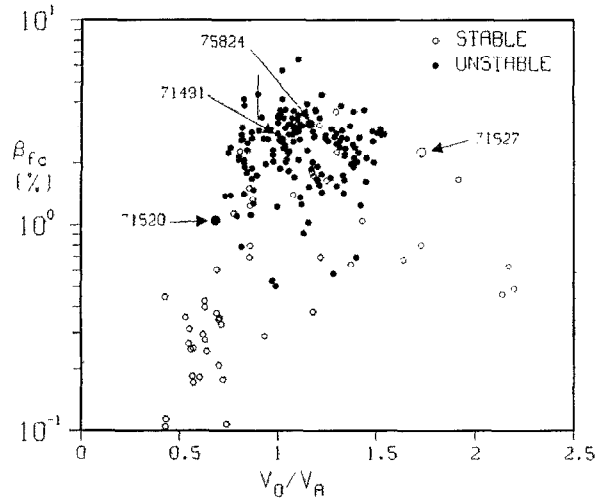

FIG. 5. Location of the discharges selected for detailed analysis in parameter space. The ordinate is the volume-averaged beam beta that would have been obtained in the absence of fast-ion losses (the classical beam beta); losses of up to 70% reduce the actual value by as much as a factor of 3 for cases with TAE activity. The abscissa is the velocity of injected full-energy beam ions normalized to the Alfvén speed. The unstable discharges had TAE activity (solid points).

$=0.52\pm0.12$ and a normalized rise and fall time of $\tau_x/T=0.20\pm0.03$. We use these values in Fig. 4 to find values of ν and a_m that are consistent with the data. If we assume $\nu=1$ (as suggested by detailed analysis of the behavior of the neutron data[18]), we find that $a_m\simeq3.0$ is consistent with both the observed value of $\Delta n/Y$ and the observed value of τ_x/T (Fig. 4). Because of the uncertainties in the experimental values, this procedure does not yield a unique solution for ν and a_m. For the PDX fishbone cycle, the data are also compatible with $\nu=2$ (Fig. 4).

Having found values of ν and a_m that are compatible with the experimental cycle, we next use Eqs. (6)–(8) to find the implied linear damping rate $\gamma_{\rm damp}$ and the particle loss rate $\gamma_{\rm loss}$. The damping rate at marginal stability is

$$\gamma_{\rm damp}=8\left(\frac{S}{\bar{N}_b}\right)(a_m-1-\ln a_m)\left(\frac{\Delta I_n}{I_n}\right)^{-2}. \tag{19}$$

The loss rate is

$$\gamma_{\rm loss}=a_m\left(\frac{S}{\bar{N}_b}\right)A_m^{-\nu}, \tag{20}$$

where A_m is the maximum value of A. For the PDX fishbone cycle, we find from Fig. 2 that $Y\simeq6$ for $a_m=3$. Substitution of the measured quantities into Eq. (19) indicates that marginal stability occurs when the beam drive $\bar{\gamma}_f=\gamma_{\rm damp}\simeq2.0\times10^4$ sec^{-1}. This value is about five times smaller than the value of $\pi\omega_{\rm pre}/4$ predicted by Chen *et al.*[16] ($\omega_{\rm pre}$ is the precession frequency) but agrees (to within a factor of 2) with the value predicted by Coppi *et al.*[17]

IV. DIII-D DATA

Intense near-tangential deuterium beam injection into low-field ($\lesssim1.4$ T) DIII-D discharges readily destabilizes TAE modes.[6] Other publications discuss the basic properties of the modes,[6] the effect of the instability upon beam-ion[19] and fusion-product[31] confinement, the observed frequencies[32] and their relationship to the theoretical gap structure,[33] and comparisons of the observations with linear stability theory.[34] For comparison, we select four discharges from data acquired during TAE mode experiments[19,34] with similar shapes ($R_0\simeq180$ cm; $a\simeq65$ cm; $\kappa\simeq1.6$; inner-wall limiter), but with markedly different nonlinear cycles. The location of the selected discharges in parameter space is shown in Fig. 5. Although none of the discharges are particularly unusual, this set of shots does provide a good sample of the variety in period, decay rate, and reduction in neutron emission that is observed. Repeated bursting is virtually always observed, although the cycle is often less reproducible than in the selected cases.

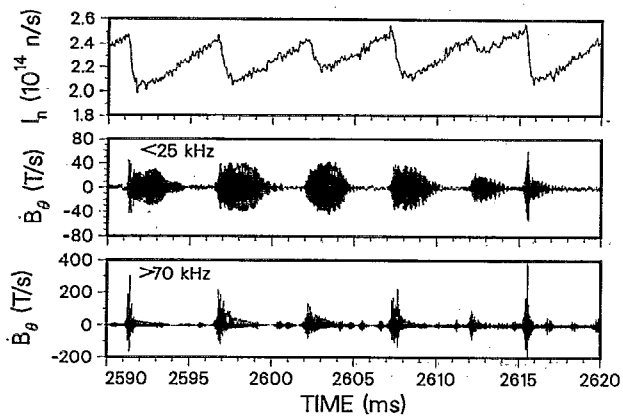

FIG. 6. Time evolution of the neutron emission and low-pass and high-pass magnetics signal in a discharge with large TAE activity (shot 75824). Here B_t=0.9 T; I_p=0.5 MA; $\bar{n}_e$=3.4×10^{13} cm^{-3}; P_b=9 MW; and β_t=3.8%. The low-pass signal is dominated by n=1 activity. The high-pass signal is due to several toroidal mode numbers with the dominant mode typically an n=6, f=98 kHz mode.

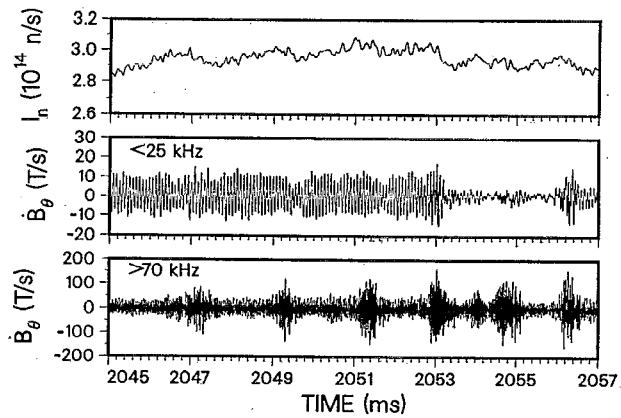

FIG. 7. Time evolution of the neutron emission and low-pass and high-pass magnetics signal in a discharge without fishbone activity (shot 71491). Here B_t=1.0 T; I_p=0.6 MA; $\bar{n}_e$=3.4×10^{13} cm^{-3}; P_b=14 MW; and β_t=2.9%. The low-pass signal is dominated by n=2 activity. The high-pass signal is due to several toroidal mode numbers with the dominant mode typically an n=4, f=73 kHz mode.

Shot 75824 (Fig. 6) is a typical discharge with TAE activity. Large bursts of MHD activity occur about every 5 msec. By digitally filtering the magnetics signal, it is evident that the activity occurs in two frequency bands: a low-frequency band below 25 kHz and a higher frequency band above 70 kHz. Fourier analysis of the magnetics and soft x-ray data shows that the low-frequency activity is caused by an n=1 fishbone mode that is nearly stationary in the plasma frame.[35] The high-frequency band is caused by a set of propagating TAE modes.[6] Occasionally small TAE bursts occur alone but, in this discharge, the large TAE bursts are all accompanied by a fishbone burst. The drop in neutron emission (15%) correlates much better with the amplitude of the TAE activity than with the fishbone amplitude, however, and this trend is generally observed in DIII-D.[19] (For example, at 2598.5 msec the slope of the neutron emission is positive, even though the amplitude of the fishbone is large.) Detailed analysis of the slope of the neutron emission, which is proportional to the rate of fast-ion loss,[18] shows that the fast-ion losses scale linearly with the TAE mode amplitude for these bursts,[19] implying that ν=1 for these conditions. The total drop in neutron emission also scales linearly with the maximum mode amplitude for these conditions, which also suggests resonant losses[19] (ν=1).

In DIII-D, TAE activity is usually accompanied by low-frequency n=1 activity, but, in roughly 20% of the discharges, fishbone and sawtooth activity are absent. In these discharges, the low-frequency band is often dominated by an n=2 mode, whose amplitude changes little on the time scale of the TAE bursts (possibly a tearing mode). Figure 7 shows shot 71491, which is an example of this behavior. In this discharge, the amplitude of the low-frequency activity is uncorrelated with the behavior of the neutron emission. Relatively large-amplitude TAE bursts occur with a period of approximately 2 msec, and these bursts correlate with small reductions in neutron emission (~3%). The reduction in mode amplitude between bursts is very modest compared to the previous case (Fig. 6). Qualitatively, this TAE cycle resembles the "run-on fishbones" occasionally observed on PDX and other tokamaks.[1]

Figure 8 shows the TAE cycle in shot 71520, which is near the high-field, low $v_\parallel/v_A$ extreme of our data set (Fig. 5). In this discharge, fishbone and TAE bursts occur simultaneously about every 7 msec, and each burst correlates with a modest drop (~4%) in neutron emission. The amplitude of both the TAE bursts and the fishbone bursts are relatively weak in this cycle. The time-dependent change in slope in the neutron emission correlates better with the instantaneous TAE amplitude than with the fishbone amplitude.

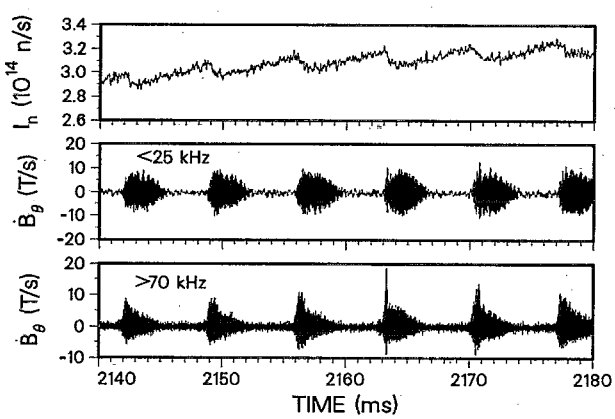

FIG. 8. Time evolution of the neutron emission and low-pass and high-pass magnetics signal in a discharge with weak TAE activity (shot 71520). Here B_t=1.4 T; I_p=0.6 MA; $\bar{n}_e$=3.0×10^{13} cm^{-3}; P_b=8 MW; and β_t=1.3%. The low-pass signal is dominated by fishbone activity and the high-pass signal is due to several toroidal mode numbers with the dominant mode typically an n=4, f=123 kHz mode.

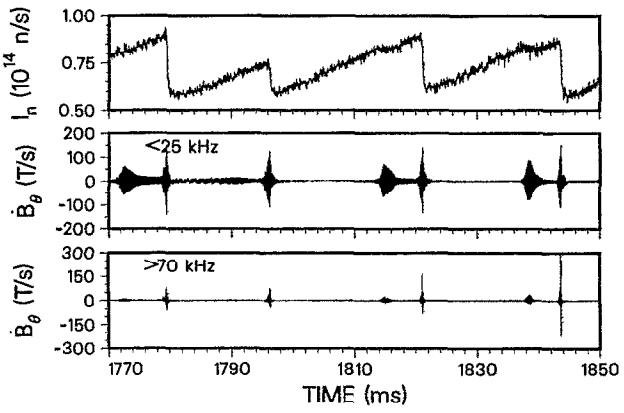

FIG. 9. Time evolution of the neutron emission and low-pass and high-pass magnetics signal in a discharge dominated by sawbone activity (shot 71527). Here B_t=0.6 T; I_p=0.6 MA; $\bar{n}_e$=3.5×10^{13} cm^{-3}; P_b=8 MW; β_t=4.5%. The low-pass signal is dominated by n=1 activity and the high-pass signal is dominated by harmonics of the n=1 activity.

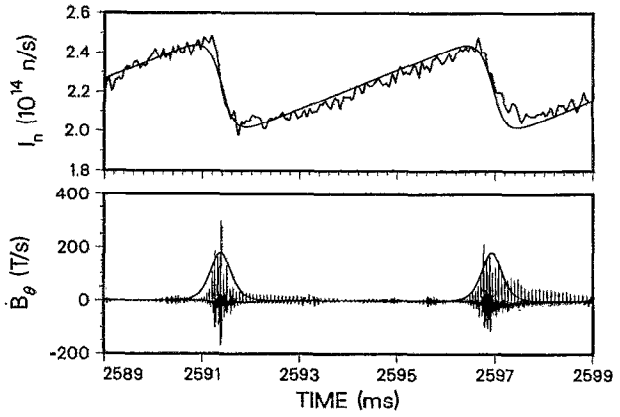

FIG. 10. Comparison of the data in Fig. 6 (jagged curves) with the solution of Eqs. (9) and (10) for ν=1 and a_m=10 (smooth curves). The magnetics data are digitally filtered to eliminate frequencies below 70 kHz.

Figure 9 shows the cycle in shot 71527, which is at the low-field, large $v_\parallel/v_A$ limit of DIII-D operation (Fig. 5). Despite intense injection of super-Alfvénic beam ions, no evidence of TAE activity is found in the Fourier spectrum of the magnetics signals for this condition. In the digitally filtered signals, high-frequency activity is apparent (Fig. 9), but the Fourier spectra of these bursts are dominated by harmonics of the low-frequency activity. The low-frequency activity consists of two types of n=1 bursts: fishbones and sawbones. The fishbone bursts (for example, at 1815 and 1838 msec) decay more gradually, have less high-frequency harmonic content, and cause a much smaller reduction in neutron emission than the sawbone events (for example, at 1821 and 1843.5 msec). The sawbone events resemble the modes observed during tangential injection into PBX.[4] The sawbones occur about every 22 msec, cause quite large drops in neutron emission (36%), and appear to dominate the nonlinear cycle (Fig. 9).

These data (Figs. 6–9) are analyzed in terms of the theoretical model of Secs. II and III. For the shots with TAE activity, we use the high-pass filtered magnetics signal to determine the rise and fall time τ_x, since the neutron signal correlates better with this signal than the low-pass signal. For the shot with sawbone bursts (71527), we use an unfiltered magnetics signal and ignore the fishbone bursts, since they have only a minor effect upon the observed cycle. The results are tabulated in Table I. The agreement with theory is good, as is illustrated in Fig. 10 for a typical case. Since the theoretical model assumes that the rise and fall times of the burst are equal, we use both

TABLE I. Analysis of experimental cycles.

			Measured quantities		
Shot	$\Delta I_n/I_n$	T (msec)	τ_x (msec)	$S/\bar{N}_b$ (sec^{-1})	$\tilde{B}_\theta/B_\theta$ (10^{-3})
PDX	0.32±0.06	2.7±0.3	0.53±0.06	230	
75824	0.15±0.05	4.8±0.8	0.38±0.30	35	1.8
71491	0.029±0.006	1.8±0.2	0.71±0.28	32	1.2
71520	0.037±0.005	7.0±0.2	1.0±0.6	10	0.06
71527	0.36±0.09	22±4	0.40±0.16	20	1.1

			Derived quantities			
Shot	$\Delta n/Y$	τ_x/T	ν	a_m	γ_{damp} (sec^{-1})	γ_{loss} (sec^{-1})
PDX	0.52±0.12	0.20±0.03	1	3	1.6e4	
			2	4.2	3.2e4	
75824	0.89±0.33	0.08±0.06	1	10	8.3e4	2e5
			2	10	8.3e4	1e8
71491	0.50±0.12	0.39±0.16	1	2.6[a]	2.0e5[a]	7e4[a]
			2	2.9	2.5e5	6e7
71520	0.53±0.07	0.14±0.09	1	4.2	1.0e5	7e5
			2	3.3	6.5e4	9e9
71527	0.82±0.27	0.018±0.007	1	20	2.0e4	4e5
			2	20	2.0e4	3e8

[a]Does not fit within error bars.

data in our calculation of τ_x, even though the fall time is often greater; in the discharges where they differ significantly, the error in τ_x is large (Table I). Also listed in Table I is the maximum amplitude of the high-pass filtered burst $\tilde{B}_\theta/B_\theta$, where $\tilde{B}_\theta$ is determined from the integral of the magnetics signal and B_θ is the poloidal field at the coil.

Using the measured quantities, we infer the parameters ν, γ_{damp}, and γ_{loss} as described in Sec. III. The results are given in Table I. In every case but the shot with the $n=2$ "tearing" mode (shot 71491), the error bars are sufficiently large that solutions with $\nu=1$, $\nu=2$, or even higher values of ν are compatible with the data. Shot 71491 is not compatible with resonant loss ($\nu=1$), however. Fortunately, the inferred marginal stability point γ_{damp} is independent of ν [Eq. (19)]. The damping rate γ_{damp} is comparable ($\sim 1.0\times 10^5$ sec^{-1}) in the two shots with combined fishbone and TAE activity (shots 75824 and 71520), while it is about a factor of 2 larger in the discharge with $n=2$ low-frequency activity. The marginal stability point in the discharge with sawbones (71527) is considerably smaller than in the TAE discharges ($\sim 2\times 10^4$ sec^{-1}), and is comparable to the damping rate found for fishbones in PDX. For both $\nu=1$ and for $\nu=2$, the loss term γ_{loss} varies considerably. (Comparing γ_{loss} for different values of ν is not physically meaningful, since the magnitude of γ_{loss} depends upon the normalization selected for the mode amplitude A.)

To assess the generality of these findings, we examine our database of DIII-D discharges with fast (500 kHz sampling) magnetics data. Nearly 100 discharges in the database have cycles dominated by repetitive, reproducible MHD bursts (which may be a combination of more than one instability). These discharges span the parameter range $B_T=0.8$–1.4 T, $I_p=0.4$–0.8 MA, $\kappa=1.1$–1.8, $\bar{n}_e=2$–5×10^{13} cm^{-3}, injected power $P_b=2$–20 MW, toroidal beta $\beta_t=1\%$–5%, and normalized beta $\beta_N=1.7$–6 (the large values of β_N are obtained with negative current ramping). Virtually all the discharges have TAE activity.

We first examine the dependence of the decay time τ_x on the normalized mode amplitude a_m. Theoretically, the decay time is expected to decrease as the mode amplitude increases [Fig. 4(a)], because large amplitude occurs when the fueling $S/\bar{N}_b$ is strong, and this results in both rapid growth and rapid quenching of the burst. Since the values of γ_{loss} and ν that convert the measured mode amplitude to a_m [Eq. (8)] are not known *a priori*, we plot τ_x/T vs $A/(S/\bar{N}_b)$ for $\nu=1$ and versus $A/\sqrt{S/\bar{N}_b}$ for $\nu=2$. We also explore various possible definitions of the mode amplitude A and of the decay time τ_x (in our theory, the rise time of the instability τ_{rise} equals the fall time τ_{fall}, but experimentally the rise and fall times often differ). The results of the analysis are shown in Fig. 11. The scatter in the data is smaller when using the average value of the rise and fall times, $\tau_x=0.5(\tau_{\text{rise}}+\tau_{\text{fall}})$ than with the definition $\tau_x=\tau_{\text{rise}}$ or $\tau_x=\tau_{\text{fall}}$. The scatter is also reduced when the measured fluctuation amplitude is normalized to the plasma current rather than to the toroidal field, i.e., $A=\tilde{B}_\theta/B_\theta$ gives a better fit than $A=\tilde{B}_\theta/B_T$. A better fit is obtained with the normalization appropriate for resonant losses

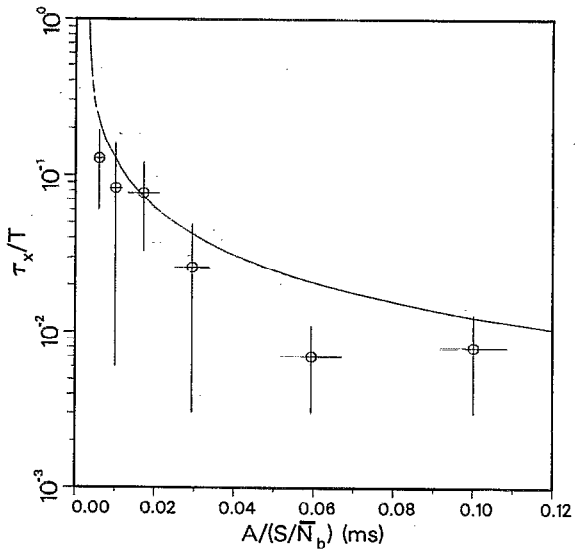

FIG. 11. Normalized decay time versus normalized mode amplitude for many discharges. The $1/e$ time τ_x is the average of the rise time of the high-pass magnetics signal τ_{rise} and the decay time τ_{fall}; only data with $\tau_{\text{fall}}<4\tau_{\text{rise}}$ are included. In the abscissa, the approximation $A\propto \dot{B}_{\text{rms}}/I_p$ is used, where $\dot{B}_{\text{rms}}$ is the average value of the high-pass signal during the burst, and the scale was normalized to $\tilde{B}_\theta/B_\theta$ for one representative case. The error bars indicate the standard deviation of many discharges. The curve is the theoretical dependence for $\nu=1$, which was fit to the data using $\gamma_{\text{loss}}=3.8\times 10^5$ sec^{-1}.

[$a_m\propto A/(S/\bar{N}_b)$ for $\nu=1$] than with the normalization appropriate for diffusive losses [$a_m\propto A^2(S/\bar{N}_b)$ for $\nu=2$]. The data show the expected tendency for the decay time to shorten as the mode amplitude increases. In plotting all the data on the same graph we are implicitly assuming that all the discharges have the same value of γ_{loss} (and ν); scatter in γ_{loss} associated with variations in mode structure presumably accounts for much of the scatter in the fit.

Theoretically, the normalized period increases gradually with increasing mode amplitude (Fig. 2). Since the value of γ_{damp} that converts the measured period T to the normalized period Y [Eq. (6)] is unknown, we consider the dependence of $T\sqrt{S/\bar{N}_b}$ upon $A/(S/\bar{N}_b)$, as in Fig. 11. Figure 12 shows the results for all discharges with $n=1$ low-frequency activity (most of the discharges in the database). The data show the expected tendency for slightly longer periods as the mode amplitude increases. By simultaneously fitting the theoretical curves in Figs. 2 and 4(a) to the data in Figs. 11 and 12, we convert the experimental abscissa to the theoretical amplitude a_m, and thereby infer the loss coefficient γ_{loss}. The curves shown in the figures imply that the average value of γ_{loss} for this data set is 3.8×10^5 sec^{-1}, in rough agreement with the values found from analysis of the individual cases (Table I). Similarly, the fit to the ordinate in Fig. 12 indicates that the average value of the marginal stability point γ_{damp} is 1.6×10^5 sec^{-1} for this data set. Presumably, the relatively large scatter in the data in Fig. 12 is associated with variation in the quantities γ_{damp} and γ_{loss} for the various plasma conditions. Inclusion of the discharges that do not have $n=1$ low-frequency bursts increases the scatter, presumably because

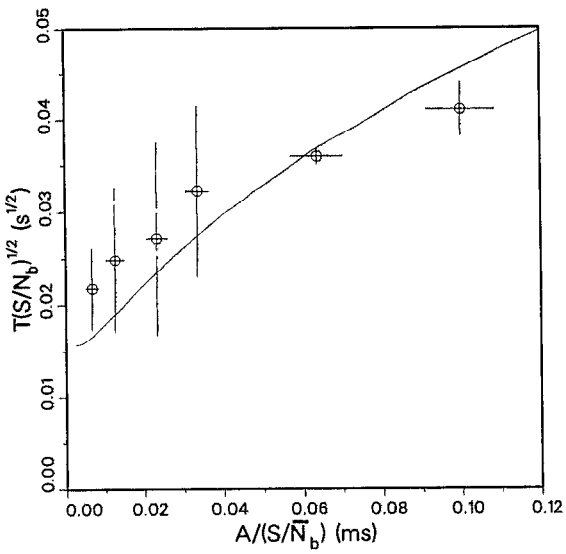

FIG. 12. Normalized period versus normalized mode amplitude for many discharges with $n=1$ low-frequency activity. The abscissa is the one employed in Fig. 11. The error bars indicate the standard deviation of many discharges. The curve is the theoretical dependence for $\nu=1$, which was fit to the data using $\gamma_{\text{loss}}=3.8\times10^5\ \text{sec}^{-1}$ and $\gamma_{\text{damp}}=1.6\times10^5\ \text{sec}^{-1}$.

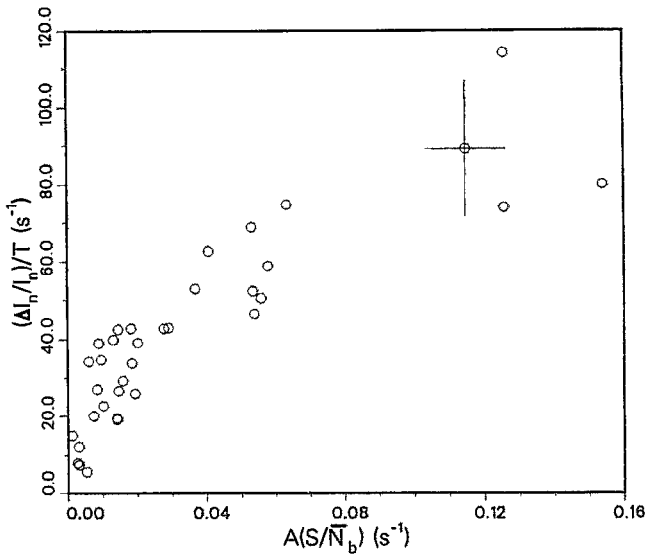

FIG. 14. Fast-ion loss rate $(\Delta I_n/I_n)/T$ versus the product of the TAE mode amplitude and the effective fueling rate $S/\bar{N}_b$ for discharges with relatively small $n=1$ low-frequency activity. The error bar shows the error for a representative discharge in the database. (Here A in the abscissa is actually $\dot{B}_{\text{rms}}/I_p$, as in Fig. 11.)

these "tearing mode" discharges increase the variation in γ_{damp} and γ_{loss} (Table I).

Theoretically, $\Delta n/Y$ assumes a value between zero and unity [Fig. 4(b)]. With the use of Eqs. (6) and (7), we see that this is equivalent to the statement that $(\Delta I_n/I_n)/T$ should not exceed the effective fueling rate $S/\bar{N}_b$. Figure 13 shows that the data in our database are consistent with this prediction. The fast-ion loss rate $(\Delta I_n/I_n)/T$ is the reciprocal of the average fast-ion confinement time.[18] Since $\bar{N}_b$ tends to clamp near the point of marginal stability, the data in Fig. 13 suggest that as the beam power is increased past the point of marginal stability (increasing S), the beam-ion confinement time degrades to preserve the condition $\bar{N}_b \simeq \text{const}$.

In summary, the duration of the burst τ_x, the period between bursts T, and the magnitude of the fast-ion losses $\Delta I_n/I_n$ are all consistent with our theoretical model.

We have also examined our data set for other relationships between the variables. Empirically, we find that the fast-ion loss rate scales with the product of the mode amplitude A and the effective fueling rate (Fig. 14). A similar correlation with $A\beta_{fc}$ is also found, where β_{fc} is the volume-average beam beta expected in the absence of fast-ion losses[19] (the classical fast-ion beta). Like Fig. 13, these empirical correlations reflect the tendency for the beam beta to saturate at the point of marginal stability.

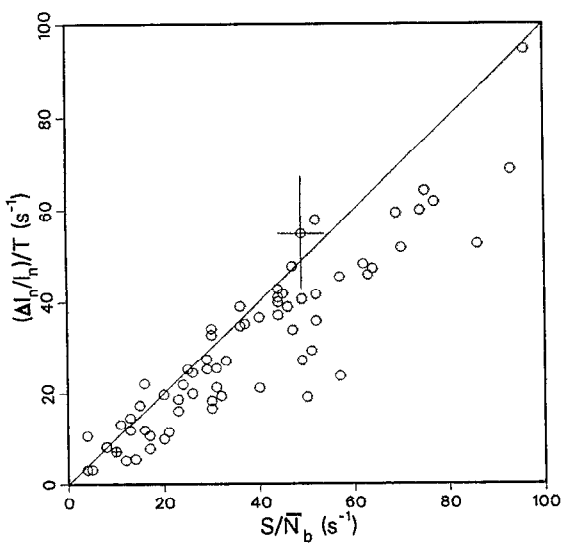

FIG. 13. Fast-ion loss rate $(\Delta I_n/I_n)/T$ versus the effective fueling rate $S/\bar{N}_b$ for many discharges. The error bar shows the error for a representative discharge in the database. Theoretically, the data should all fall below the diagonal line.

V. DISCUSSION

Analysis of the observed nonlinear cycle yields the mode damping rate γ_{damp} [Eq. (19)]. Measurements of the temperature, density, and current profiles of the plasma permit an independent calculation of the expected damping of TAE modes. Use of approximate formulas for the ion and electron damping,[36] coupling to kinetic Alfvén waves,[37] and continuum damping[38] yield a value of $\gamma_{\text{damp}}\simeq5\times10^4\ \text{sec}^{-1}$ for a discharge similar to 71520 and 71527, with an estimated accuracy of no better than a factor of 2.[34] The value of γ_{damp} inferred from the nonlinear cycle is $\sim8\times10^4\ \text{sec}^{-1}$ (Table I), so the two methods are in reasonable agreement.

Another check on the model is the inferred value of the particle-loss coefficient ν. The observed nonlinear cycles for plasmas with low-frequency $n=1$ activity are consis-

tent with $\nu \geqslant 1$, with the best fit to the data in Fig. 11 implying $\nu \simeq 1$. This is consistent with independent analysis of the scaling of $\Delta I_n/I_n$ with A at individual bursts,[19] as well as with Langmuir probe measurements that imply resonant beam-ion losses.[19]

The model also predicts that the beam beta clamps near the point of marginal stability, as observed experimentally.[19]

There are interesting differences between discharges with $n=1$ low-frequency activity and discharges with saturated tearing modes (or kinks) with $n>1$. Both the inferred value of γ_{damp} and the inferred value of ν tends to be higher in the latter discharges, while γ_{loss} tends to be smaller (Table I). Perhaps the changes in current profile that govern the transition in low-frequency MHD activity also increase the damping of TAE modes. A possible explanation for the change in particle losses is that combined $n=1$ and TAE activity can resonantly transport particles all the way from the plasma center to the plasma edge, while TAE activity alone is less effective at particle transport. Studies of the drop in neutron emission $\Delta I_n/I_n$ versus the TAE mode amplitude A indicate that combined TAE and fishbone activity cause larger losses than TAE activity alone.[19]

In the stability diagram of Fig. 5, it is somewhat surprising that some discharges with $v_0/v_A > 1$ such as shot 71527 do not exhibit TAE activity. Analysis of the nonlinear cycle provides the explanation. In these very low-field discharges, the marginal stability point for $n=1$ activity occurs at the relatively low value of $\gamma_{\text{damp}} \simeq 2\times 10^4\ \text{sec}^{-1}$ (Table I). This causes the beam beta to saturate below the threshold for TAE activity (which occurs for $\gamma_{\text{damp}} \simeq 8\times 10^4\ \text{sec}^{-1}$). In other words, at a very low field the violent losses associated with sawbone activity prevent excitation of TAE modes.

The only significant discrepancy between our theory and experiment is in the evolution of the mode amplitude. In our model, the rise and fall of the mode amplitude is symmetric with respect to time. In the experiment, the fall time almost always exceeds the rise time of the TAE instability. (This was also the case for the fishbone instability in PDX.[39]) In our model, we assume that the mode structure, background damping rate, beam-ion gradient, and beam-ion velocity distribution remain constant throughout a burst. Presumably, changes in one or more of these quantities during the burst accounts for the asymmetric evolution of the mode amplitude.

Our model equations do not address the initial growth of the unstable mode, but represent the oscillations about the nonlinear steady state. Although we have compared γ_{damp} with the linear damping rate, our basic equations apply even if nonlinear effects modify the damping, as long as γ_{damp} remains constant in time. In our model, since the basic equations are conservative, the system oscillates indefinitely once the initial conditions are established. The actual plasma almost certainly contains some dissipation, however, so one might expect the oscillations to damp to the marginal stability point ($a_m \to 1$). Indeed, more realistic model equations[28,40] are dissipative. There may even be experimental evidence that the cycle decays; for example, the fishbone cycle in Fig. 1 of Ref. 2 does decay slightly between sawtooth crashes (both $\Delta I_n/I_n$ and T decrease), although the changes may be caused by changes in q (or other plasma parameters). What then prevents the cycle from decaying, and why are oscillations virtually always observed? A likely answer is that other instabilities, such as the sawtooth instability, perturb the plasma and reestablish initial conditions for the oscillatory cycle. In mathematical terms, a more realistic model would contain stochastic differential equations rather than deterministic ones, or would contain one or more additional evolution equations (for the amplitudes of other instabilities) that are coupled with the beam-ion equation [Eq. (10)]. Experimentally, irregular bursting is often observed when several instabilities are present. Periodic cycles are observed most often when one instability is dominant, although occasionally a pair of instabilities (such as TAE bursts and sawbones) will alternate repetitively. Borba *et al.* recently showed that inclusion of a forcing term in Eq. (5) (to simulate the effect of other instabilities) can produce period doubling and complex, irregular bursting.[41]

VI. CONCLUSION

A semiempirical model for the nonlinear "saturation" of fast-ion-driven instabilities through the loss of fast ions was extended and solved. Instabilities with discrete, well-separated modes that expel the driving particles at low mode amplitude are governed by these equations. In particular, the model applies to most fast-ion-driven instabilities, including fishbones, TAE modes, EAE modes, and kinetic ballooning modes.

Application of the model to TAE modes in DIII-D gives good agreement with the experimental observations. Although the model fails to reproduce exactly the detailed evolution of the mode amplitude within a burst, it succeeds in predicting all the gross features of the nonlinear cycle, including (i) the clamping of the beam beta near the point of marginal stability, (ii) the dependence of the fast-ion losses upon the beam fueling, (iii) the gradual increase in the period between bursts as the beam power increases, (iv) the shortening of the duration of the burst as the beam power increases, (v) a linear damping rate in rough agreement with theory, and (vi) resonant losses ($\nu=1$) during $n=1$ low-frequency activity.

In light of these successes, we conclude that particle loss controls the saturation of TAE modes in DIII-D.

These findings imply that it will not be possible to operate a reactor above the marginal stability point of alpha-driven instabilities. Attempts to drive the plasma past the marginal stability point will merely increase the alpha losses. Since the losses associated with fishbones and TAE modes are concentrated poloidally, the escaping alphas threaten damage (erosion, sputtering, impurity influx, etc.) to the inside walls without affording any appreciable benefit to the plasma performance. Prudence therefore dictates that reactors operate at or below the threshold for instability. Future studies should concentrate on efforts to raise the damping rate of the relevant insta-

bilities to increase the stable operating regime. For example, efforts to enhance continuum damping of TAE modes through current profile control[34,42] may prove useful.

ACKNOWLEDGMENTS

Useful discussions with B. Breizman, L. Chen, R. Goldston, M. Rosenbluth, N. Rostoker, and R. White and the support of the DIII-D team are gratefully acknowledged.

This work was supported by Subcontract No. SC-L134501 of U.S. Department of Energy Contract No. DE-AC03-89ER51114.

[1]W. W. Heidbrink and G. Sadler, "The behavior of fast ions in tokamak experiments," Nucl. Fusion (in press).

[2]K. McGuire, R. Goldston, M. Bell, M. Bitter, K. Bol, K. Brau, D. Buchenauer, T. Crowley, S. Davis, F. Dylla, H. Eubank, H. Fishman, R. Fonck, B. Grek, R. Grimm, R. Hawryluk, H. Hsuan, R. Hulse, R. Izzo, R. Kaita, S. Kaye, H. Kugel, D. Johnson, J. Manickam, D. Manos, D. Mansfield, E. Mazzucato, R. McCann, D. McCune, D. Monticello, R. Motley, D. Mueller, K. Oasa, M. Okabayashi, K. Owens, W. Park, M. Reusch, N. Sauthoff, G. Schmidt, S. Sesnic, J. Strachan, C. Surko, R. Slusher, H. Takahashi, F. Tenney, P. Thomas, H. Towner, J. Valley, and R. White, Phys. Rev. Lett. **50**, 891 (1983).

[3]S. von Goeler, W. Stodiek, and N. Sauthoff, Phys. Rev. Lett. **33**, 1201 (1974).

[4]W. W. Heidbrink, K. Bol, D. Buchenauer, R. Fonck, G. Gammel, K. Ida, R. Kaita, S. Kaye, H. Kugel, B. LeBlanc, W. Morris, M. Okabayashi, E. Powell, S. Sesnic, and H. Takahashi, Phys. Rev. Lett. **57**, 835 (1986).

[5]K. L. Wong, R. J. Fonck, S. F. Paul, D. R. Roberts, E. D. Fredrickson, R. Nazikian, H. K. Park, M. Bell, N. L. Bretz, R. Budny, S. Cohen, G. W. Hammett, F. C. Jobes, D. M. Meade, S. S. Medley, D. Mueller, Y. Nagayama, D. K. Owens, and E. J. Synakowski, Phys. Rev. Lett. **66**, 1874 (1991).

[6]W. W. Heidbrink, E. J. Strait, E. Doyle, G. Sager, and R. Snider, Nucl. Fusion **31**, 1635 (1991).

[7]Y. M. Li, S. M. Mahajan, and D. W. Ross, Phys. Fluids **30**, 1466 (1987).

[8]R. Betti and J. P. Friedberg, Phys. Fluids B **3**, 1865 (1991).

[9]H. Biglari and L. Chen, Phys. Rev. Lett. **67**, 3681 (1991).

[10]L. Chen, in *Theory of Fusion Plasmas*, Proceedings of the Joint Varenna–Lausanne International Workshop, Chexbres, 1988 (Editrice Compositori, Bologna, 1989), p. 327.

[11]G. Y. Fu and J. W. Van Dam, Phys. Fluids B **1**, 1949 (1989). Note that ω_{*f} in this reference is defined at one-half the birth energy, rather than at the full energy, as in Eq. (1).

[12]C. Z. Cheng, Phys. Fluids B **3**, 2463 (1991).

[13]H. L. Berk, B. N. Breizman, and H. Ye, Phys. Rev. Lett. **68**, 3563 (1992).

[14]H. Biglari and P. H. Diamond, Phys. Fluids B **4**, 3009 (1992).

[15]F. Gang, Phys. Fluids B **4**, 3152 (1992).

[16]L. Chen, R. B. White, and M. N. Rosenbluth, Phys. Rev. Lett. **52**, 1122 (1984).

[17]B. Coppi, S. Migliuolo, and F. Porcelli, Phys. Fluids **31**, 1630 (1988).

[18]J. D. Strachan, B. Grek, W. W. Heidbrink, D. Johnson, S. M. Kaye, H. W. Kugel, B. LeBlanc, and K. McGuire, Nucl. Fusion **25**, 863 (1985).

[19]H. H. Duong, W. W. Heidbrink, T. W. Petrie, E. J. Strait, R. L. Lee, R. A. Moyer, and J. G. Watkins, "Loss of beam ions during TAE instabilities," Nucl. Fusion (in press).

[20]D. S. Darrow, E. D. Fredrickson, H. E. Mynick, R. Nazikian, R. B. White, K.-L. Wong, and S. J. Zweben, in *Proceedings of the 19th European Conference on Plasma Physics and Controlled Fusion*, Innsbruck, 1992 (Commission of the European Communities, Brussels, 1992).

[21]K. L. Wong, R. Durst, R. J. Fonck, S. F. Paul, D. R. Roberts, E. D. Fredrickson, R. Nazikian, H. K. Park, M. Bell, N. L. Bretz, R. Budny, C. Z. Cheng, S. Cohen, G. W. Hammett, F. C. Jobes, L. Johnson, D. M. Meade, S. S. Medley, D. Mueller, Y. Nagayama, D. K. Owens, S. Sabbagh, and E. J. Synakowski, Phys. Fluids B **4**, 2122 (1992).

[22]J. Luxon, P. Anderson, F. Batty, C. Baxi, G. Bramson, N. Brooks, B. Brown, B. Burley, K. H. Burrell, R. Callis, G. Campbell, T. Carlstrom, A. Colleraine, J. Cummings, L. Davis, J. DeBoo, S. Ejima, R. Evanko, H. Fukomoto, R. Gallix, J. Gilleland, T. Glad, P. Gohil, A. Gootgeld, R. J. Groebner, S. Hanai, J. Haskovec, E. Heckman, M. Heiberger, F. J. Helton, P. Henline, D. Hill, D. Hoffman, E. Hoffman, R. Hong, N. Hosogane, C. Hsieh, G. L. Jackson, G. Jahns, G. Janeschitz, E. Johnson, A. Kellman, J. S. Kim, J. Kohli, A. Langhorn, L. Lao, P. Lee, S. Lightner, J. Lohr, M. Mahdavi, M. Mayberry, B. McHarg, T. McKelvey, R. Miller, C. P. Moeller, D. Moore, A. Nerem, P. Noll, T. Ohkawa, N. Ohyabu, T. Osborne, D. Overskei, P. Petersen, T. Petrie, J. Phillips, R. Prater, J. Rawls, E. Reis, D. Remsen, P. Riedy, P. Rock, K. Schaubel, D. Schissel, J. Scoville, R. Seraydarian, M. Shimada, T. Shoji, B. Sleaford, J. Smith, Jr., P. Smith, T. Smith, R. T. Snider, R. D. Stambaugh, R. Stav, H. St. John, R. Stockdale, E. J. Strait, R. Street, T. S. Taylor, J. Tooker, M. Tupper, S. K. Wong, and S. Yamaguchi, in *Plasma Physics and Controlled Nuclear Fusion Research, 1986* (International Atomic Energy Agency, Vienna, 1987), Vol. I, p. 159.

[23]R. B. White, R. J. Goldston, K. McGuire, A. H. Boozer, D. A. Monticello, and W. Park, Phys. Fluids **26**, 2958 (1983).

[24]D. J. Sigmar, C. T. Hsu, R. White, and C. Z. Cheng, Phys. Fluids B **4**, 1506 (1992).

[25]R. Kaita, R. B. White, A. W. Morris, E. D. Fredrickson, K. M. McGuire, S. S. Medley, T. J. Murphy, and S. D. Scott, Phys. Fluids B **2**, 1584 (1990).

[26]A. Rescigno and I. W. Richardson, in *Foundations of Mathematical Biology*, edited by R. Rosen (Academic, New York, 1973), Vol. III, Chap. 4.

[27]Equation (C8) of Ref. 17 should read as $\bar{n}_h = \pm\{(\Gamma^2/2)[1-\exp(2N_h)+2N_h]+(\Delta\bar{n}_h)^2\}^{1/2}$ and the denominator of the integrand in Eq. (C10) should equal $\bar{n}_h$.

[28]R. B. White, *Theory of Tokamak Plasmas* (North-Holland, Amsterdam, 1989), p. 280.

[29]P. Beiersdorfer, R. Kaita, and R. J. Goldston, Nucl. Fusion **24**, 487 (1984).

[30]D. Buchenauer, W. W. Heidbrink, L. Roquemore, and K. McGuire, Rev. Sci. Instrum. **58**, 2264 (1987).

[31]H. H. Duong and W. W. Heidbrink, Nucl. Fusion **33**, 211 (1993).

[32]E. J. Strait, W. W. Heidbrink, and A. D. Turnbull, "Behavior of the TAE mode frequency in DIII-D," submitted to Plasma Phys. Controlled Fusion.

[33]A. D. Turnbull, E. J. Strait, W. W. Heidbrink, M. S. Chu, H. H. Duong, J. M. Greene, L. L. Lao, T. S. Taylor, and S. J. Thompson, Phys. Fluids B **5**, 2546 (1993).

[34]E. J. Strait, W. W. Heidbrink, A. D. Turnbull, M. S. Chu, and H. H. Duong, "Stability of neutral beam driven TAE modes in DIII-D," submitted to Nucl. Fusion.

[35]W. W. Heidbrink and G. Sager, Nucl. Fusion **30**, 1015 (1990).

[36]R. Betti and J. P. Friedberg, Phys. Fluids B **4**, 1465 (1992).

[37]R. R. Mett and S. M. Mahajan, Phys. Fluids B **4**, 2885 (1992).

[38]M. N. Rosenbluth, H. L. Berk, J. W. Van Dam, and D. M. Lindberg, Phys. Rev. Lett. **68**, 596 (1992).

[39]D. Buchenauer, Ph.D. thesis, Princeton University, 1985.

[40]For example, the evolution equation $dN_b/dt = S - \gamma_{\rm loss} A^{\nu} N_b$, which makes the losses proportional to the instantaneous beam number N_b rather than the average number $\bar{N}_b$, is dissipative. The reasonable assumption that the losses are delayed by a slight amount ϵ with respect to the mode amplitude (due to the finite transit time of the beam ions), $dN_b/dt = S - \gamma_{\rm loss} A(t-\epsilon)\bar{N}_b$, also results in a damped cycle.

[41]D. Borba, M. F. F. Nave, and F. Porcelli (private communication, 1992).

[42]K. L. Wong (private communication, 1992).